Chemical Communications

Dynamic Article Links ▶

Cite this: DOI: 10.1039/c0xx00000x

www.rsc.org/xxxxxx

Communications

Kinetic and Thermodynamic of Metal Binding to the N-terminus of Human Copper Transporter, hCTR1

Xiubo Du, Hongyan Li, Xinghao Wang, Qiong Liu, Jiazuan Ni and Hongzhe Sun (e-mail: hsun@hku.hk)

Sample preparation

The GB1-tagged wild-type hCTR1_*N* and its mutants (GB1-WT, GB1-MutA, GB1-MutB and GB1-MutC, for sequences see Fig. S1) were expressed and purified as described previously.[1] hCTR1_*N* and its variants were isolated from the tagged proteins via Factor Xa cleavage followed by a two-step purification with Ni^{2+}-IMAC and size exclusion chromatography.

Protein samples were analyzed by SDS-PAGE (13%, Tris-Glycine running buffer) and visualized with Coomassie Blue R-250 (Fig S2-A). Band corresponding to hCTR1_*N* was digested with Chymotrypsin (Sigma) at 37 ^{o}C overnight. Peptide fragments were then analyzed with matrix assisted laser desorption ionization-mass spectrometry (MALDI-MS) and compared with theoretically digested peptides calculated by MS-digest software.

ESI mass spectra were recorded on Finnigan LCQ Deca (Thermo) mass spectrometer with a capillary voltage set at 27 V and sample flow rate of 5 µl/min. Purified proteins were prepared in ammonium bicarbonate buffer (5 mM, pH 8.0) and diluted to ca. 20 µM. Equal volume of methanol was added to the protein solution and acetic acid was used to adjust pH to 3. Parameters used in mass experiments were as followed: spray voltage, 4.6 kV; capillary temp., 200 ^{o}C; number of scan, 50; sheath gas flow rate, 90.

The identities of both wild-type and muant hCTR1_*N* were confirmed by MALDI-TOF-MS (Fig S2-B) and ESI-MS (Fig S3).

Cu^{+} Titration

UV-Vis spectra were recorded on a Varian Cary 3E UV-visible spectrophotometer with a 1-cm cuvette at room temperature. Cu^{+} titration experiment was carried out under anaerobic condition. Briefly, apo-protein (20 µM) in 20 mM MES/Tris buffer, pH 8.5 was thoroughly de-oxygenated and transferred to the cuvette sealed with a septum cap. Aliquots of 1 mM $[Cu(MeCN)_4]PF_6$ dissolved in de-oxygenated acetonitrile were titrated into the cuvette using an airtight syringe. The absorption spectra were monitored over the wavelength range of 200-800 nm, and normalized with the absorbance at 800 nm.

Circular Dichroism Spectroscopy

Circular dichroism experiments were carried out in a 0.1-cm-pathlength quartz cell on a Jasco J-720 spectropolarimeter calibrated with 0.06% (+)-10-camphorsulphonic acid solution (Sigma-Aldrich). CD spectra of 60 µM apo- or Cu-bound hCTR1_*N* in 5 mM ammonium bicarbonate buffer (pH 8.5) were recorded. The spectra were baseline-corrected by substracting the corresponding buffer spectra obtained under identical condition and smoothed using a fast Fourier transform (FFT) filter.

Estimation of Cu^{+} Binding Constants

Bicinchoninic acid is a colorimetric Cu^{+} chelator, which can form a stable purple complex with Cu^{+} in a 2:1 ratio as $[Cu(BCA)_2]^{3-}$ that exhibits absorption maxima at 562 nm (ε= 7900 $M^{-1}\cdot cm^{-1}$) and 358 nm (ε= 42 900 $M^{-1}\cdot cm^{-1}$).[2] Therefore, the transfer of Cu^{+} from BCA to protein was evaluated by monitoring the changes in UV-Vis absorbance of $Cu(BCA)_2$ at 562 nm. At the wavelength between 450 nm and 650 nm, neither apo- nor copper-bound proteins gave any absorption, while UV absorption from BCA occurs at $\gamma \leq 370$ nm.

Experiments of competition reaction between the protein and BCA were carried out under anaerobic conditions as described previously.[3] Briefly, Cu^{+} solutions in the form of $[Cu(MeCN)_4]PF_6$ were mixed with BCA in a molar ratio of 1:3 in MES/Tris buffer (20 mM, pH 8.5) as a stock solution. Protein solutions at various concentrations were then mixed with the stock solution to give rise to a final concentration of Cu^{+} of 27 µM and BCA of 84 µM. Ascorbic acid was kept at 0.8 mM to maintain the oxidation state of Cu^{+} in the reaction mixture. To ensure the equilibrium to be reached, the mixture was incubated at room temperature for at least 1 hour (no additional change in absorption was observed). The results were corrected for dilution and base-line absorbance at 800 nm.

The absorbance data obtained in hCTR1_*N* titrated into $[Cu(BCA)_2^{3-}]$ (Fig. S7-B) were used to calculate the binding constants for Cu^{+}-hCTR1_*N* complexes, using the following equations.

$$Cu(BCA)_2 + P = (Cu-P) + 2BCA$$

$$K_{a1} = \frac{[Cu-P][BCA]^2}{[Cu(BCA)_2][P]} \quad \text{(Eq.1)}$$

$$Cu(BCA)_2 + (Cu-P) = (Cu_2-P) + 2BCA$$

$$K_{a2} = \frac{[Cu_2-P][BCA]^2}{[Cu(BCA)_2][Cu-P]} \quad \text{(Eq.2)}$$

$$\cdots\cdots$$

$$Cu(BCA)_2 + (Cu_{n-1}-P) = (Cu_n-P) + 2BCA$$

$$K_{an} = \frac{[Cu_n-P][BCA]^2}{[Cu(BCA)_2][Cu_{n-1}-P]} \quad \text{(Eq.3)}$$

$$Cu^{+} + 2BCA^{2-} = Cu(BCA)_2^{3-}$$

$$\beta_2 = \frac{[Cu(BCA)_2]}{[Cu][BCA]^2} \quad \text{(Eq.4)}$$

β_2 is the associated constant of $Cu(BCA)_2$ and two different values (4.6×10^{14} and 2.0×10^{17})[2, 3] were reported previously. The former was obtained by ITC and it was considered to underestimate the affinity between Cu^+ and the chelator due to the diminished heat release as a result of conversion of $Cu(I)Cl_n$ species to $Cu(I)(BCA)_2$. Here we chosed the later value which was also used to calculate the Cu^+ binding constants of several other Met-containing Cu transporters or chaperones, such as CopK, CopC, PcoC and CusF.

Here we assumed that the n binding sites for Cu^+ on hCTR1_*N* are independent and equivalent. We take n=2 first and then generalize the result to cases for which n >2.

The relationships between the equilibrium constants K_{a1} and K_{a2} and the stablity constants for Cu^+-hCTR1_*N* (K_1 and K_2) and the association constant for $Cu(BCA)_2$ (ß$_2$) are given by the following equations.

$$Cu + P = Cu - P$$
$$K_1 = \frac{[Cu-P]}{[Cu][P]} = \beta_2 \cdot K_{a1} \quad \text{(Eq.5)}$$
$$Cu + (Cu-P) = Cu_2 - P$$
$$K_2 = \frac{[Cu_2-P]}{[Cu][Cu-P]} = \beta_2 \cdot K_{a2} \quad \text{(Eq.6)}$$

The fractional saturation Y=(concentration of Cu bound to P)/(total concentration of all forms of P), that is

$$Y = \frac{[Cu-P]+2[Cu_2-P]}{[P]+[Cu-P]+[Cu_2-P]} \quad \text{(Eq.7)}$$

Rearranging Eqs 1, 2 and 7 results in Eq. 8:

$$Y = \frac{\frac{K_{a1}[P]}{X} + \frac{2K_{a2}}{X}\cdot\frac{K_{a1}[P]}{X}}{[P] + \frac{K_{a1}[P]}{X} + \frac{K_{a2}}{X}\cdot\frac{K_{a1}[P]}{X}} = \frac{\frac{K_{a1}}{X} + \frac{2K_{a2}}{X}\cdot\frac{K_{a1}}{X}}{1 + \frac{K_{a1}}{X} + \frac{K_{a2}}{X}\cdot\frac{K_{a1}}{X}} = \frac{\frac{2K_a}{X} + \frac{2K_a^2}{X^2}}{1 + \frac{2K_a}{X} + \frac{K_a^2}{X^2}} = \frac{\frac{2K_a}{X}}{1+\frac{K_a}{X}} = \frac{2K_a}{X+K_a} \quad \text{(Eq.8)}$$

Where $X = \frac{[BCA]^2}{[Cu(BCA)_2]}$, K_a is the intrinsic binding constants, and K_{a1}=2K_a and K_{a2}=K_a/2 from statistic point of view. Therefore:

$$\frac{1}{Y} = \frac{1}{2} + \frac{1}{2K_a}\cdot X \quad \text{(Eq.9)}$$

Eq. 9 is the result obtained for two equivalent sites. In general, for n equivalent sites, it can be written in:

$$\frac{1}{Y} = \frac{1}{n} + \frac{1}{nK_a}\cdot X \quad \text{(Eq.10)}$$

The slopes of the plot of 1/Y versus X gave log K_a = -2.38 ± 0.04 (correlation coefficient r = 0.99, n= 2.81) for WT, log K_a = -3.11 ± 0.05 (correlation coefficient r = 0.96, n= 1.85) for MutA and log K_a = -2.42 ± 0.05 (correlation coefficient r = 0.94, n= 1.08) for WT. The binding numbers obtained from the data fitting are in good agreements with those obtained from UV-titration. Using the known value for the association constant of $Cu(BCA)_2$ of log ß$_2$ = 17.30, binding constants of log K_{WT} =14.92, log K_{MutA} = 14.19 and log K_{MutB} = 14.88 were calculated for Cu^+ hCTR1_*N* variants.

Chemical Modification of hCTR1_*N* with Diethylpyrocarbonate (DEPC)

To modify the histidine residues of hCTR1_*N*, 100 molar equivalents of DEPC (freshly diluted in absolute ethanol) were added to 0.05 mM of hCTR1_*N* in 20 mM Na_2HPO_4 / NaH_2PO_4 buffer, pH 7.4. The mixture was stirred at room temperature for 3 hrs, and excess DEPC was then removed by dialysis. The number absorbance of N-carbethoxyimidazole at 240 nm with known $\Delta\varepsilon_{240}$ of 3200 M^{-1} cm^{-1}.[4]

Kinetics of Cu^+ Exchange Between hCTR1_*N* and BCA

Kinetics of Cu^+ Binding

Cu^+ in the form of $[Cu(MeCN)_4]PF_6$ was mixed with BCA in a molar ratio of 1:3 under anaerobic conditions in 20 mM MES/Tris buffer at pH 8.5 as a stock solution. Ascorbic acid of 1 mM was supplied to maintain the Cu^+ oxidation state in the reaction mixture. hCTR1_*N* with various final concentrations were then added to the stock solution to give the final concentration of Cu^+ of 30 µM and BCA of 90 µM and the protein of 0, 125, 188, 250 and 313 µM. Kinetics of Cu^+ binding to hCTR1_*N* was monitored by the absorbance change at 562 nm using a Varian Cary 3E UV-Vis spectrophotometer.

Kinetics of Cu^+ Release

Five molar equivalents of Cu^+ (as $[Cu(MeCN)_4]PF_6$) were added to 100 µM of hCTR1_*N* under anaerobic conditions in 50 mM MES/Tris buffer, 1 mM ascorbic acid, pH 8.0. After incubation at room temperature for an hour, excess Cu^+ ions were removed from the protein by a PD-10 desalting column. BCA with final concentrations of 0, 25, 75, 100 and 1000 µM was added to the Cu^+ bound hCTR1_*N* and the absorbance change at 562 nm was recorded using a Varian Cary 3E UV-Vis spectrophotometer.

All kinetics data were fitted to a first-order reaction function.

Isothermal Titration Calorimetry (ITC)

ITC measurements were performed on a MicroCal iTC-200 microcalorimeter (Northampton, MA) at 25 °C. The purified proteins were treated with 10 mM EDTA for 3 hours and then subjected to three rounds of dialysis against appropriate buffer. The titrant was made by mixing appropriate amounts of stock solution of metal ions (20 mM $AgNO_3$ or 10 mM $CuSO_4$ in nanopure Milli-Q water) with a buffer retained from the final dialysis of the protein sample. The metal concentration of the stock solution was determined by ICP-MS.

Briefly, 2 µl of 1.5-3 mM $AgNO_3$ or $CuSO_4$ were titrated into 200 µl of 24-110 µM proteins over 4 s with a 3-min interval between each injection. Twenty injections were made in total. The reaction solution was stirred at 1000 rpm. The heat of dilution, mechanical effects and non-specific interactions were accounted for by averaging the last three points of titration and the value was subtracted from all data points. The results were analyzed by Origin 7.0 (Microcal) using either one-site binding or sequential binding model. A nonlinear least square method was used to obtain the best fit parameters for the number of binding sites, n, the association constant, K_a, and the change of enthalpy

ΔH. All of the experiments were performed in trplicate under the same conditions.

Ag^+ binding to hCTR1_*N* examined by Equilibrium Dialysis and ICP-MS

Binding of Ag^+ to the wild-type hCTR1_*N* and its mutants were investigated via equilibrium dialysis with the metal concentrations determined by ICP-MS (Inductively coupled plasma mass spectrometry). The proteins (ca. 100 µl at 20 µM) in 20 mM MES/Tris buffer, pH 7.4, were dialyzed using 3 kDa cut-off mini-dialysis kit (Amersham Biosciences) against the same buffer supplemented with a series of concentrations of $AgNO_3$ ranging from 0 to 80 µM at 4 ℃ overnight. The Ag^+ concentrations inside and outside the dialysis tubes were measured by ICP-MS. Each measurement was performed in trplicate.

The results were analyzed by Origin 7 Hill function using the one-site binding model, which gave rise to the maximal binding capacity of 3.48±0.33 and the dissociation constant (K_d) of (7.17±1.99) µM for the wild-type protein (Fig. S8). Under the same conditions, MutA and MutB were found to bind (2.36±0.20) and (1.17±0.09) Ag^+ ions per monomer of the protein, with the dissociation constants of (14.66±2.60) and (10.60±1.67) µM, respectively. No specific binding was observed in the case of MutC. (due to the high deviation of K_d=(5.01±1305.9) µM)

Estimation of Buffer-independent Cu^{2+} Binding Constants

Cu^{2+} binding to hCTR1_*N* variants were studied by ITC at 25 ℃ in 20 mM *N*-(2-acetamido)-2-aminoethanesulfonic acid (ACES; pH 7.4) and 100 mM NaCl. ACES was chosen not only for its buffering capacity at the desired pH, but also for the formation of the well-defined $Cu^{2+}(ACES)_2$ complex. A recently reported method was used to extract buffer-independent binding constants.[5] The K_{ITC} equation is shown as:

$$K_{ITC} = \frac{[P-2Cu^{2+}]}{[P]_{ITC}([Cu^{2+}]_{ITC})^2} \quad (1)$$

where $[P]_{ITC}$ and $[Cu^{2+}]_{ITC}$ represent the fractions of protein and Cu^{2+} that are not found in the metal-protein complex, respectively.

$$\begin{aligned}[Cu^{2+}]_{ITC} &= [Cu^{2+}]_C - 2[P-2Cu^{2+}] \\ &= [Cu^{2+}]+[ACES-Cu^{2+}]+[2ACES-Cu^{2+}] \\ &+[ACES-Cu^{2+}-(H_{-1}ACES)]+[2(H_{-1}ACES)-Cu^{2+}]\end{aligned} \quad (2)$$

where $[Cu^{2+}]_C$ represents total Cu^{2+} concentration.

The pH 7.4 requirement restricts the analysis to a single peptide protonation state as represented by Eq. 3:

$$[P]_{ITC} = [P] \quad (3)$$

The expressions that represent the various metal-buffer equilibria (Eqs. 4-7) and the buffer-independent *K* expression (Eq. 8) required for the analysis are listed below. Log *K* and log ß values can be found in the reference.

$$K_{MB} = \frac{[ACES-Cu^{2+}]}{[Cu^{2+}][ACES]}; (\log K = 4.32) \quad (4)$$

$$K_{MB2} = \frac{[2ACES-Cu^{2+}]}{[ACES]^2[Cu^{2+}]}; (\log ß = 7.77) \quad (5)$$

$$K_{M(H_{-1}B)B} = \frac{[2ACES-Cu^{2+}]}{[H][ACES-Cu^{2+}-H_{-1}ACES]}; (\log K = 7.36) \quad (6)$$

$$K_{M(H_{-1}B)_2} = \frac{[2ACES-Cu^{2+}]}{[H]^2[2H_{-1}ACES-Cu^{2+}]}; (\log ß = 15.34) \quad (7)$$

$$K_{P-2Cu^{2+}} = \frac{[P-2Cu^{2+}]}{[Cu^{2+}]^2[P]} \quad (8)$$

Rearranging Eqs 1, 3 and 8 results in Eq 9:

$$K_{p-2Cu^{2+}} = K_{ITC}\left(\frac{[Cu^{2+}]_{ITC}}{[Cu^{2+}]^2}\right)^2 \quad (9)$$

Substituting Eq 2 and Eqs 4-7 into Eq 9 results in Eq 10:

$$\begin{aligned}K_{P-2Cu^{2+}} = K_{ITC}(1+K_{MB}[ACES]+K_{MB_2}[ACES]^2 + \\ \frac{K_{MB_2}}{K_{M(H_{-1}B)B}}\frac{[ACES]^2}{[H]}+\frac{K_{MB_2}}{K_{M(H_{-1}B)_2}}\frac{[ACES]^2}{[H]^2})^2\end{aligned} \quad (10)$$

Substituting the value of K_{ITC} into Eq 10 provided the buffer-independent binding constant (K) and dissociation constant (K_d).

Reference

1. X. Wang, X. Du, H. Li, D. S. Chan and H. Sun, *Angew Chem Int Ed Engl*, 2011, **50**, 2706-2711.
2. Z. Xiao, P. S. Donnelly, M. Zimmermann and A. G. Wedd, *Inorg Chem*, 2008, **47**, 4338-4347.
3. L. A. Yatsunyk and A. C. Rosenzweig, *J Biol Chem*, 2007, **282**, 8622-8631.
4. P. S. Jois, N. Madhu and D. N. Rao, *Biochem J*, 2008, **410**, 543-553.
5. N. E. Grossoehme, A. M. Spuches and D. E. Wilcox, *J Biol Inorg Chem*, 2010, **15**, 1183-1191.

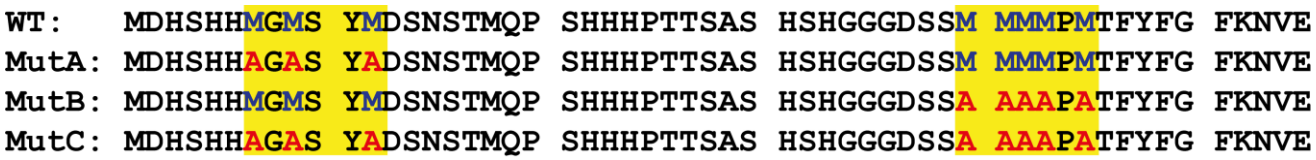

Fig. S1 Protein sequences of the wild-type and mutant hCTR1_*N*. The two methionine-rich motifs are highlighted in yellow. Met and Ala residues in these motifs are shown as blue and red, respectively.

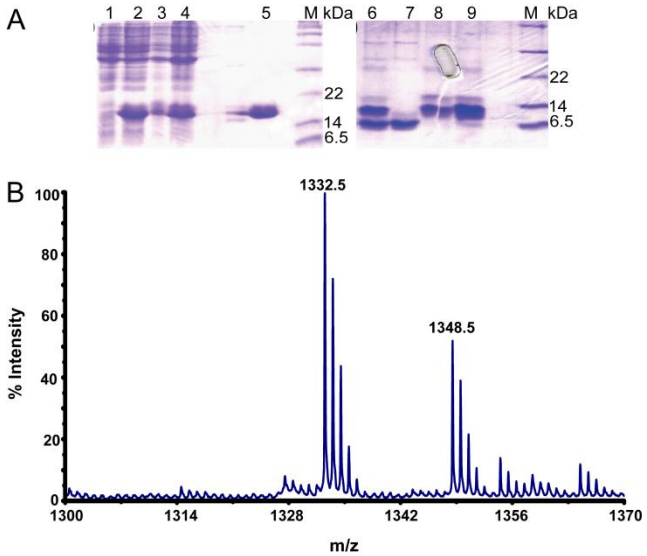

Fig. S2 (A) SDS-PAGE showing the expression and purificiation of hCTR1_N. lane 1, non-induced cell extract; lane 2, IPTG-induced cell extract; lane 3, pellets; lane 4, supernatant; lane 5, purified GB1-hCTR1_N; lane 6, GB1-hCTR1_N cut with Factor Xa and the digested products were applied to Ni^{2+}-IMAC; lane 7, flow-through, corresponding to GB1 tag; lane 8, elutes with 120 mM imidazole, corresponding to hCTR1_N; lane 9, hCTR1_N purified with gel filtration.
(B) MALDI-TOF-MS analysis of hCTR1_N digested with chymotrypsin.
The spectrum revealed two major peaks at m/z 1332.5 and 1348.5 respectively, corresponding to the N-terminal peptide MDHSHHMGMSY of hCTR1_N (calc, 1332.49, and 1348.48 with oxidation).

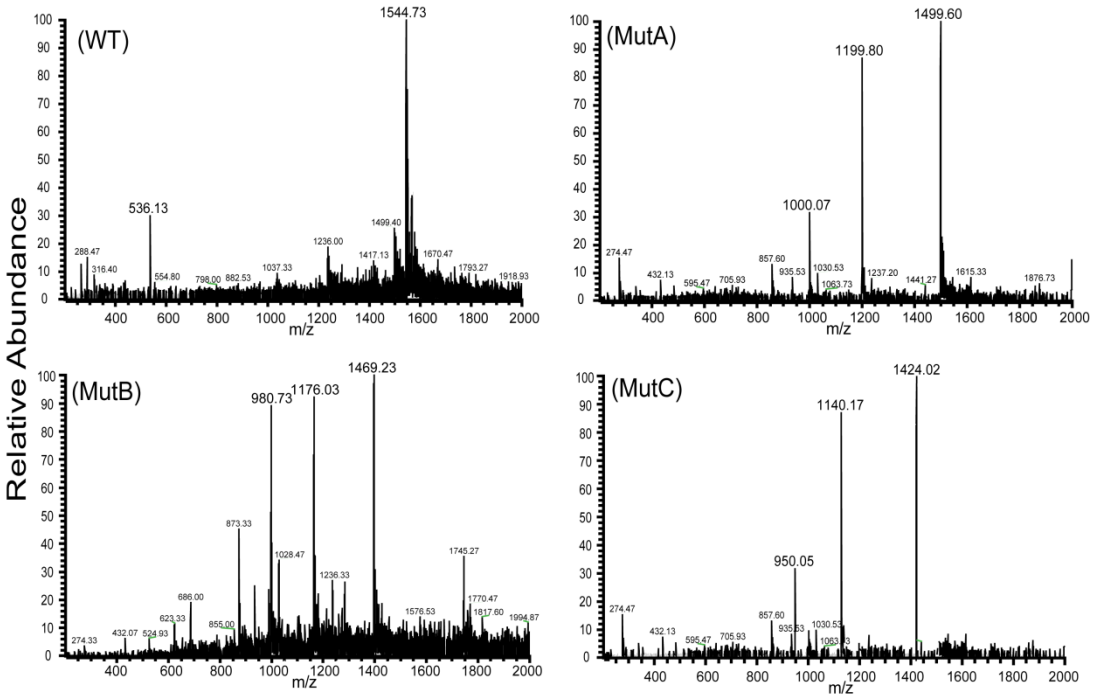

Fig.S3 ESI-MS analysis of the wild-type and mutant hCTR1_*N*. Spectrum of the wild-type protein showed two peaks at m/z 1544.73 and 1236.00, corresponding to +4 and +5 charged proteins (calc, 1544.97 and 1236.17, respectively). Spectra of mutant proteins revealed peaks at m/z: 1499.60, 1199.80 and 1000.07, corresponding to +4, +5 and +6 charged MutA (calc, 1499.88, 1200.11 and 1000.26); 1469,23, 1176.03 and 980.73, corresponding to +4, +5 and +6 charged MutB (calc, 1469.83, 1176.06 and 980.22); 1424.02, 1140.17 and 950.05, corresponding to +4, +5 and +6 charged MutC (calc, 1424.74, 1139.99 and 950.16).

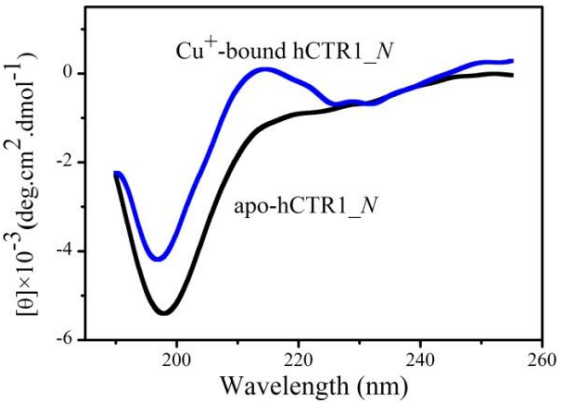

Fig. S4 Circular dichroism spectra of apo- and Cu^{+}- bound hCTR1_*N* (60 μM) in 5 mM ammonium bicarbonate buffer, pH 8.5.

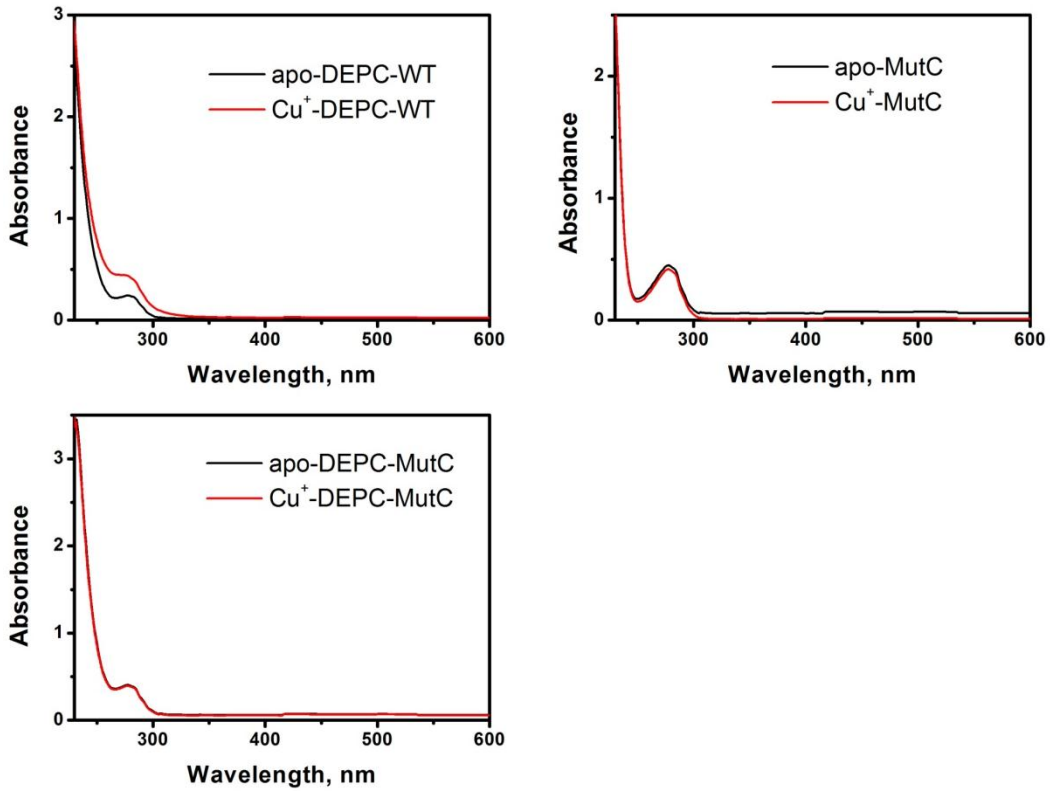

Fig. S5 UV-visible spectra of DEPC-WT, MutC and DEPC-MutC with the addition of 1 equiv $[Cu^{1}(CH_3CN)_4]^+$ in 50 mM MES/Tris buffer at pH 8.5.

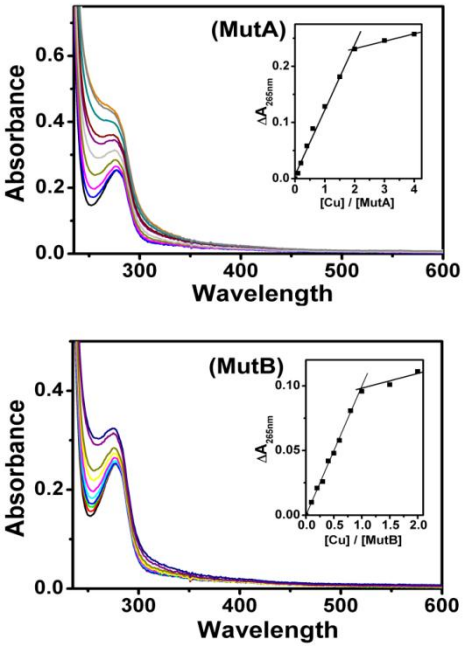

Fig. S6 UV-visible spectra of MutA and MutB proteins titrated with $[Cu^{1}(CH_3CN)_4]^+$ (1.6 mM) in 50 mM MES/Tris buffer at pH 8.5. *Inserts*: Plots of absorbance at 265 nm versus Cu/protein ratio, indicative of 2.0 and 1.0 Cu^+ binding to MutA and MutB respectively.

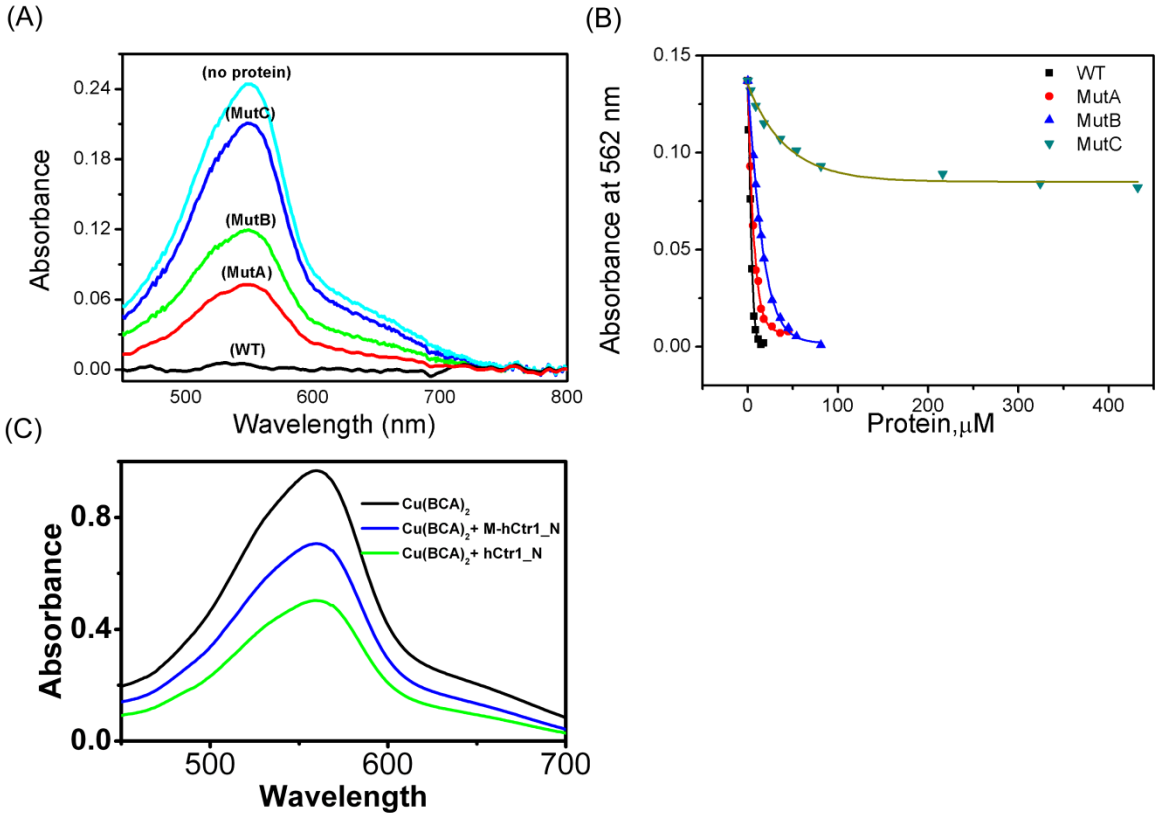

Fig. S7 (A) UV_vis spectra of Cu (27 μM), ascorbate (0.8 mM) and BCA (84 μM), with the addition of hCTR1_*N* variants. (B) Titration of hCTR1_*N* variants into 27 μM Cu^{+}, 84 μM BCA and 0.8 mM ascorbate. (C) Effects of DEPC modification on Cu^{+} binding to hCTR1_*N*. UV-vis absorption spectra of 125 μM $Cu(BCA)_2$ (—), 125 μM $Cu(BCA)_2$ incubated with 0.5 mM hCTR1_*N* (—), or with 0.5 mM DEPC modified hCtr1_N (—) for one hour. Experiments were carried out in 20 mM MES/Tris buffer, pH 8.0, at 25 °C.

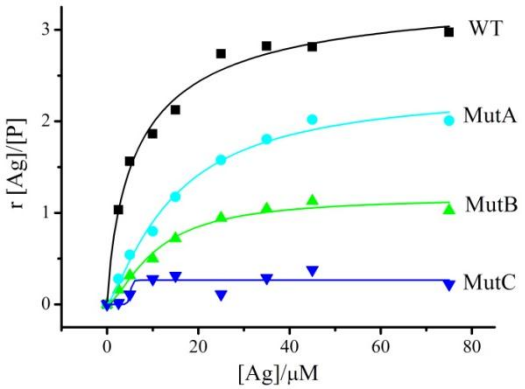

Fig. S8 Binding profiles of Ag^+ to hCTR1_*N* and its variants by equilibrium dialysis. The proteins at 20 μM were dialyzed against the same buffer supplemented with $AgNO_3$ concentrations ranging from 0 to 80 μM at 4 °C overnight. The graphs show Hill plots of the molar ratios of bound Ag^+ to proteins against concentrations of $AgNO_3$ in the dialysis buffer.

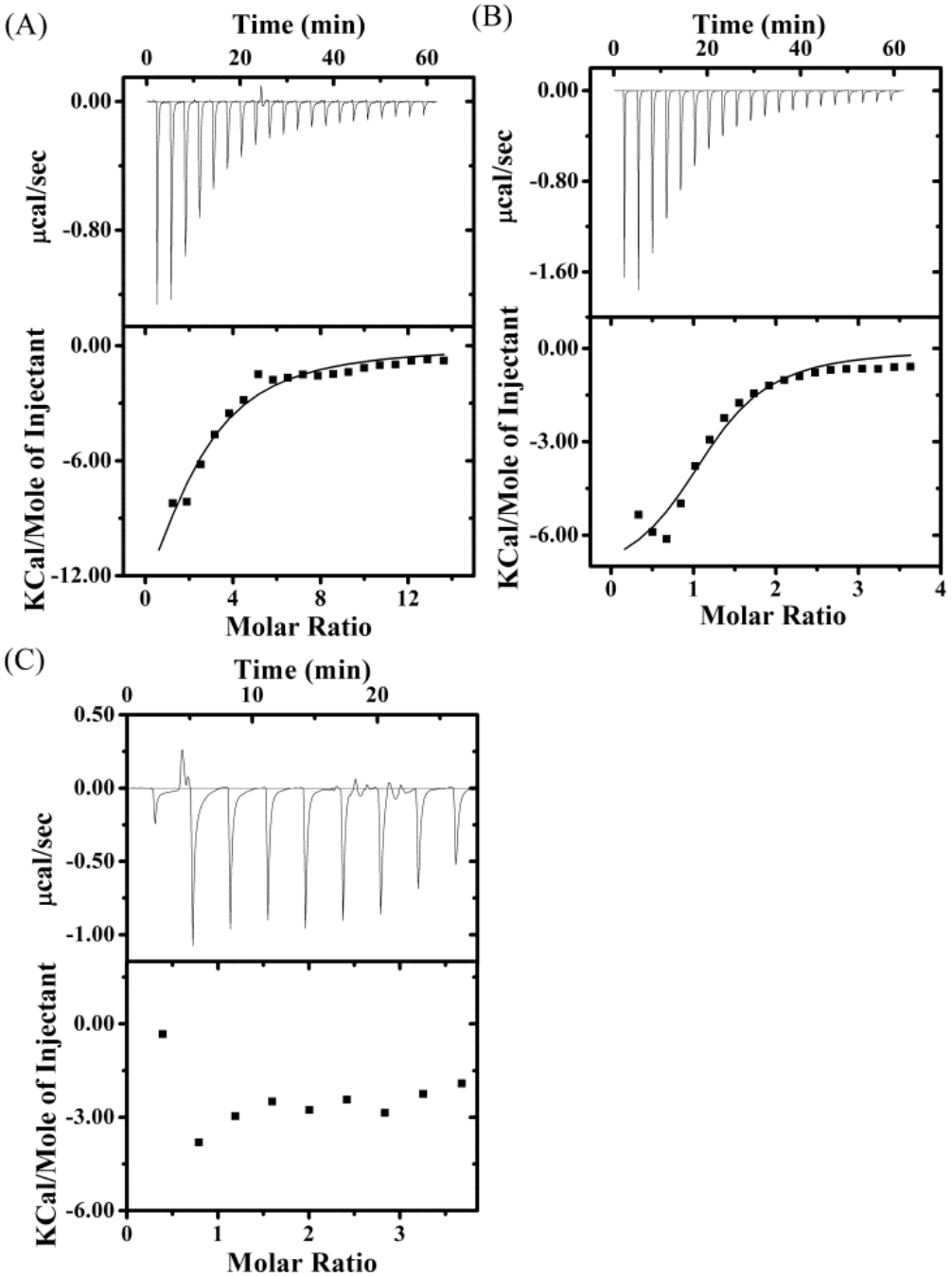

Fig. S9 Calorimetric titration of Ag^+ to hCTR1_*N* variants. Top, raw data. Bottom, plots of integrated heat versus the Ag/protein ratio. The solid line represents the best fit using single binding site model (A) 24 µM MutA titrated with 1.5 mM $AgNO_3$ (B) 110 µM MutB titrated with 2 mM $AgNO_3$ (C) 81 µM MutC titrated with 3 mM $AgNO_3$. All experiments were carried out in 50 mM MES/Tris buffer, pH 8.0, at 25 ^oC.

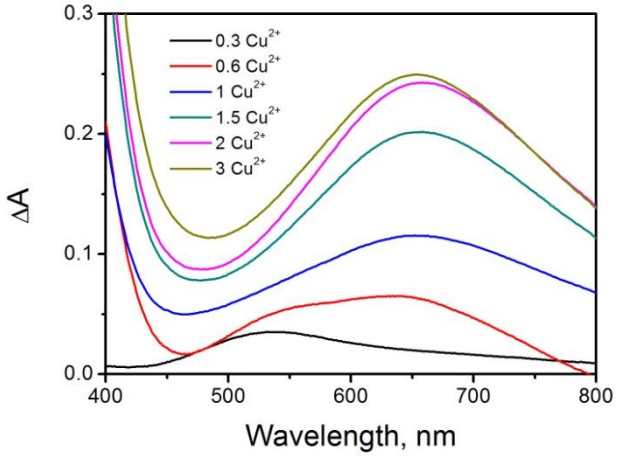

Fig. S10 Difference UV-visible spectra of hCTR1_*N* (100 µM) titrated with $CuSO_4$ in 50 mM Tris buffer, pH 7.4.

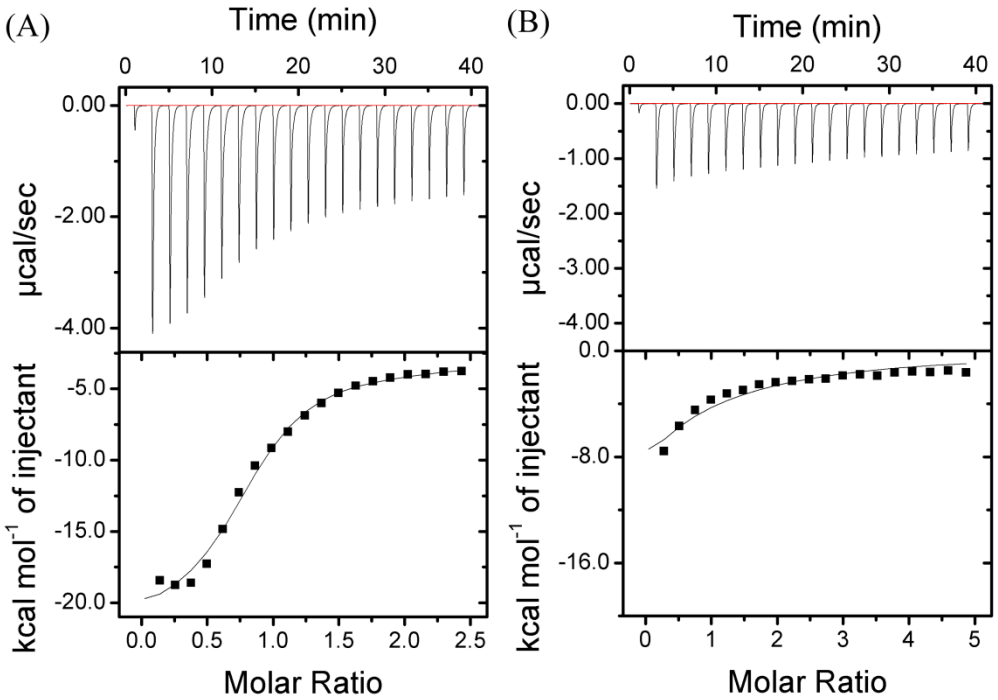

Fig. S11 Calorimetric titration of Cu^{2+} to hCTR1_*N* variants. *Top*, raw data; *Bottom*, plots of integrated heat versus the Cu/protein ratio. The solid line represents the best fit with single binding site model (A) 90 µM MutC titrated with 2 mM $CuSO_4$ (B) 45 µM His-modified MutC titrated with 2 mM $CuSO_4$. All experiments were carried out in 50 mM ACES buffer, pH 7.4, at 25 ^{o}C.

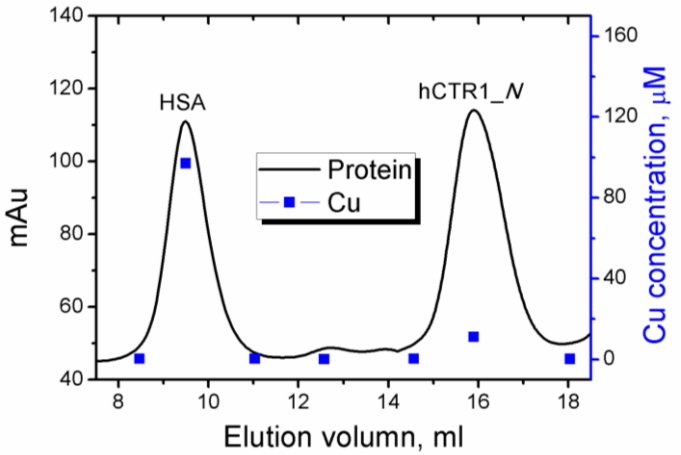

Fig. S12 Transfer of Cu^{2+} from HSA to hCTR1_*N*. apo- hCTR1_*N* was incubated with 1 equiv $(Cu^{2+})_2$-HSA for 1 h before analysis by gel filtration on a Superdex 75 column. The concentration of Cu^{2+} was determined by ICP-MS.

Table S1 Best-fit thermodynamic parameters of metal ions binding to hCTR1_*N* and its variants obtained from ITC measurements.

		N_{ITC}	K_{ITC} ($\times 10^4$)	ΔH_{ITC} [kcal mol^{-1}]	ΔS_{ITC} [cal mol^{-1} K]	K ($\times 10^9$)
Ag^+	WT	2.9±0.1	1.8±0.1	-19.3±0.1	-38.5	
	MutA	2.0±0.1	47.6±18.1	-23.1±1.1	-57.7	
	MutB	1.2±0.1	21.3±2.7	-7.6±0.1	-4.06	
Cu^{2+}	WT	1	25.8±5.9	-13.5±1.3	-20.5	3.7±0.9
		1	1.7±0.5	51.3±6.7	191	0.26±0.08
	MutC	1	13.9±1.6	-21.2±0.5	-47.5	2.0±0.2
		1	0.3±0.1	17.1±6.9	73.4	0.04±0.01